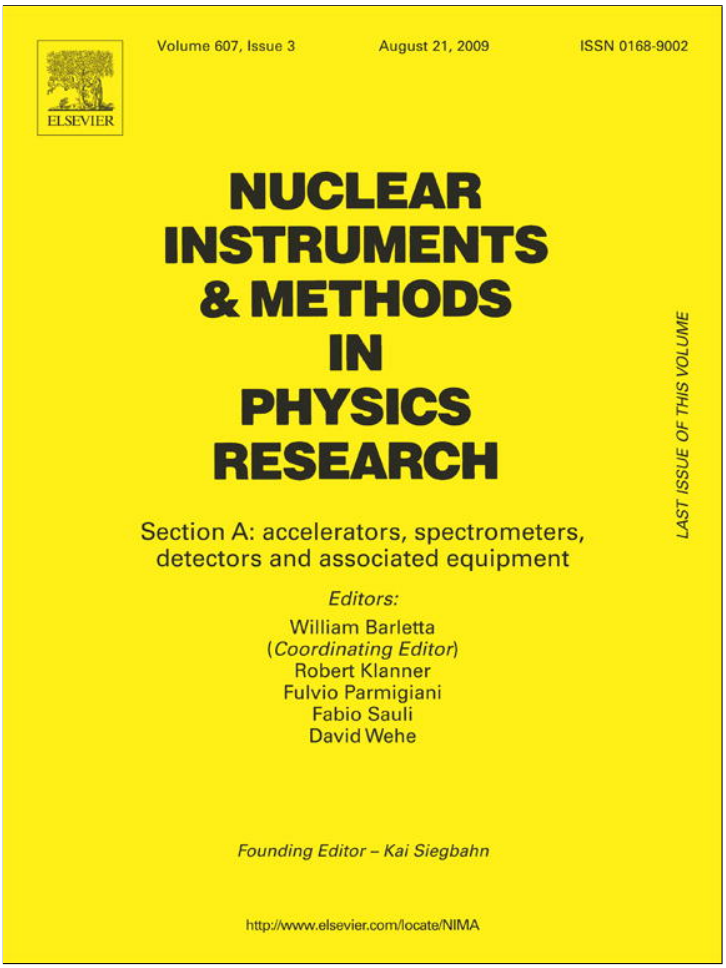

Nuclear Instruments and Methods in Physics Research A 607 (2009) 568–572

Contents lists available at ScienceDirect

Nuclear Instruments and Methods in Physics Research A

journal homepage: www.elsevier.com/locate/nima

Absolute ^{60}Co characterization based on gamma–gamma coincident detection by two NaI(Tl) detectors

Peter Volkovitsky [a,*], Philip Naudus [b]

[a] National Institute of Standards and Technology, Gaithersburg, MD 20899, United States
[b] George Mason University, Fairfax, VA

ARTICLE INFO

Article history:
Received 16 January 2009
Received in revised form
19 May 2009
Accepted 4 June 2009
Available online 11 June 2009

Keywords:
NaI(Tl) detector
Absolute calibration
Coincidence gamma-rays
^{60}Co isotope

ABSTRACT

A gamma–gamma coincidence measurement method was used for the characterization of ^{60}Co. A two-dimensional analysis of coincident events allows the careful calculation of the number of counts, when each of the two γ-rays emitted by ^{60}Co is in the photopeak area in each of the NaI(Tl) detectors. The standard formulas that were applied for absolute calibration of ^{125}I (Eldridge–Crowther formulas) were modified for the case of ^{60}Co decay. These modified Eldridge–Crowther formulas were applied to the absolute calibration of ^{60}Co samples measured by the two NaI(Tl) detectors both in coincidence and normal modes. Measurements were performed for three sources of different activities and for two positions of each source between the two NaI(Tl) detectors. Results are in good agreement with the measurements of the same samples done by the 4πβ-γ method.

Published by Elsevier B.V.

1. Introduction

Photon–photon coincidence counting is one of only a few ways to make direct measurements of activity in radioactive decays [1–3]. This method is widely used for the characterization of ^{125}I by detection of X-ray–γ-ray coincident events [4–10]. Because of the low energies of both X-rays and γ-rays in ^{125}I decay (27, 31 and 35 keV), only photopeaks contribute to the observed spectra. Let us consider ^{125}I source between the two NaI(Tl) detectors. An NaI(Tl) detector cannot discriminate X-rays with energies 27 and 31 keV from a γ-ray with energy 35 keV. Following [5], the count rate N_i in detector i ($i=1,2$) under the photopeak (which includes both X-rays and γ-rays) can be written as:

$$N_i = N_0[\varepsilon_i^{(1)}(1-\varepsilon_i^{(2)}) + \varepsilon_i^{(2)}(1-\varepsilon_i^{(1)})], \quad (1)$$

where N_0 is the disintegration rate of ^{125}I and $\varepsilon_i^{(j)}$ the probability of detection of the photon j ($j=1,2$) by the detector i. In the case of ^{125}I probabilities $\varepsilon_i^{(j)}$ are products of full peak detection efficiencies (which coincide with total detection efficiencies) by emission probabilities. $(1-\varepsilon_i^{(j)})$ is the probability that the photon j is not detected by the detector i.

The coincident count rate (count rate of events detected simultaneously by both detectors) can be written as

$$N_c = N_0(\varepsilon_1^{(1)}\varepsilon_2^{(2)} + \varepsilon_1^{(2)}\varepsilon_2^{(1)}) \quad (2)$$

Using the notations of [5], $\varepsilon_1^{(2)} = K_1\varepsilon_1^{(1)} = K_1\varepsilon_1$ and $\varepsilon_2^{(2)} = K_2\varepsilon_2^{(1)} = K_2\varepsilon_2$. Then Eqs. (1) and (2) can be written as

$$N_i = N_0[(1+K_i)\varepsilon_i - 2K_i\varepsilon_i^2] \quad (3)$$

and

$$N_c = N_0(K_1+K_2)\varepsilon_1\varepsilon_2. \quad (4)$$

If the two detectors are identical, then $K_1 = K_2 = K$ and Eqs. (3) and (4) can be written as

$$N_1 = N_0[(1+K)\varepsilon_1 - 2K\varepsilon_1^2] \quad (5a)$$

$$N_2 = N_0[(1+K)\varepsilon_2 - 2K\varepsilon_2^2] \quad (5b)$$

$$N_c = 2N_0K\varepsilon_1\varepsilon_2. \quad (5c)$$

Probabilities ε_1 and ε_2 may be eliminated from Eqs. (5a)–(5c) and the disintegration rate N_0 can be expressed in terms of N_1, N_2 and N_c:

$$N_0 = \frac{2K}{(1+K)^2}\frac{(N_1N_2 - N_c^2)^2}{N_c(N_1-N_c)(N_2-N_c)}. \quad (6)$$

Eq. (6) is equivalent to Eq. (13) from [5].

For ^{125}I spectra, the low-energy photopeak in the NaI(Tl) detector partially overlaps with the summation peak at a higher energy. Because of this, it is more convenient to measure each detector's total count rate $\tilde{N}_i$

$$\tilde{N}_i = N_0[\varepsilon_i^{(1)}(1-\varepsilon_i^{(2)}) + \varepsilon_i^{(2)}(1-\varepsilon_i^{(1)}) + \varepsilon_i^{(1)}\varepsilon_i^{(2)}]. \quad (7)$$

* Corresponding author. Tel.: +1 301 975 5527; fax: +1 301 926 7416.
E-mail address: peter.volkovitsky@nist.gov (P. Volkovitsky).

0168-9002/$ - see front matter Published by Elsevier B.V.
doi:10.1016/j.nima.2009.06.002

The last term in brackets is the contribution from the summation peak. In this case, the disintegration rate is equal to

$$N_0 = \frac{2K}{(1+K)^2}\frac{(\tilde{N}_1\tilde{N}_2 - N_c^2/4)^2}{N_c(\tilde{N}_1 - N_c/2)(\tilde{N}_2 - N_c/2)}. \quad (8)$$

Eq. (8) is equivalent to Eq. (7) from [5].

2. Formulas for ^{60}Co decay

There have been many attempts to apply coincident detection for absolute characterization of isotopes that emit coincident γ-rays of higher energies, in particular for ^{60}Co with two coincident γ-rays with energies 1173 and 1332 keV [11–15]. For ^{60}Co decay, the branching of the cascade decay $4^+ \rightarrow 2^+ \rightarrow 0^+$ with coincident emission of two γ-rays is close to 100% (99.90%, see [16]).

The direct generalization of Eqs. (1)–(4), however, meets with some difficulties. The count rate under photopeak j ($j = 1, 2$) in detector i ($i = 1, 2$) is equal to

$$N_i^{(1,p)} = N_0\varepsilon_i^{(1,p)}(1 - \varepsilon_i^{(2,tot)}) \quad (9a)$$

$$N_i^{(2,p)} = N_0\varepsilon_i^{(2,p)}(1 - \varepsilon_i^{(1,tot)}), \quad (9b)$$

where N_0 is the disintegration rate of ^{60}Co into the channel with two coincident γ-rays and $N_i^{(j,p)}$ the count rate in the detector i of events in the photopeak of the γ-ray j. $\varepsilon_i^{(j,p)}$ is the probability of γ-ray j detection in the photopeak by detector i and is equal to the full peak efficiency multiplied by the γ-ray j emission probability. $\varepsilon_i^{(j,tot)}$ is the total probability of detecting γ-ray j by detector i, including Compton scattered γ-rays and is equal to the total efficiency multiplied by the emission probability for γ-ray j. $(1-\varepsilon_i^{(j,tot)})$ is the probability that γ-ray j is not detected by the detector i.

The first difference between the description of ^{60}Co and ^{125}I decays arises because of the Compton scattering contribution. The total detection efficiency is different from the full peak detection efficiency, and for ^{60}Co the number of unknown probabilities is twice as many as for the ^{125}I case. Another problem relates to the careful account of the coincident events. Because of these problems, a summation method, which does not require the coincident count rate detection, was mainly applied for ^{60}Co [17–20]. Below we will present formulas for the coincident count rate in the two detectors and will calculate the activity of the ^{60}Co source.

There is a summation peak $N_i^{(1,2)}$ in each detector i

$$N_i^{(1,2)} = N_0\varepsilon_i^{(1,p)}\varepsilon_i^{(2,p)} \quad (10)$$

and two peaks of coincident events in both detectors, where the energies deposited in each detector are in the single photopeak areas

$$N_c^{(1,2)} = N_0\varepsilon_1^{(1,p)}\varepsilon_2^{(2,p)} \quad (11a)$$

$$N_c^{(2,1)} = N_0\varepsilon_1^{(2,p)}\varepsilon_2^{(1,p)}. \quad (11b)$$

In Eq. (11a) $N_c^{(1,2)}$ is the count rate of coincident events for which the first γ-ray is detected by the first detector and the second γ-ray is detected by the second detector; similarly in Eq. (11b) $N_c^{(2,1)}$ is the count rate of coincident events for which the second γ-ray is detected by the first detector and the first γ-ray is detected by the second detector.

The coincident events may be presented by a three-dimensional histogram on a two-dimensional plane (see Fig. 1). One horizontal axis is proportional to the energy deposited in the first detector, and another horizontal axis is the energy deposited in the second detector.

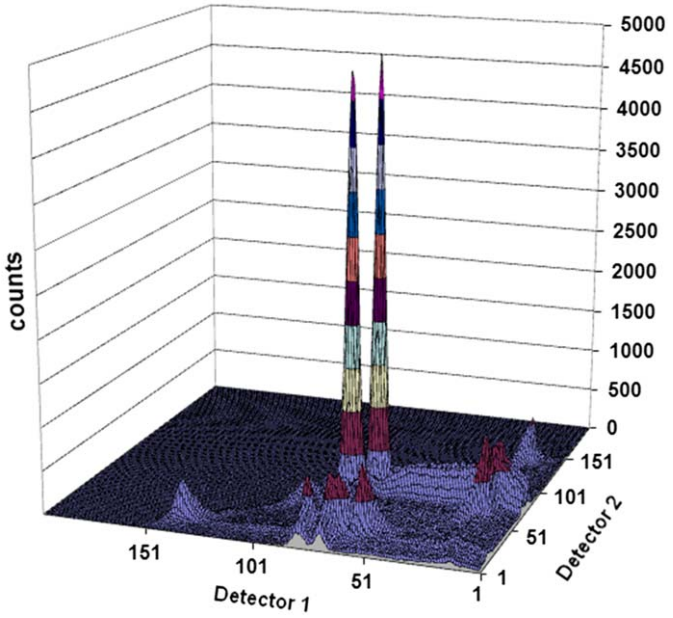

Fig. 1. Two-dimensional spectrum for source C3 in the middle position. Channel 1 was assigned to the top detector; channel 2 was assigned for the bottom detector. Compton tails are clearly seen for each detector.

The projections of coincident events onto each horizontal axis are one-dimensional coincident spectra (see Fig. 2). There are four projections of two coincident peaks.

The count rate of coincident events in the first detector, $N_{1c}^{(1,p)}$, when the first γ-ray is detected in the area of the photopeak and the second γ-ray with any energy is detected by the second detector, can be written as

$$N_{1c}^{(1,p)} = N_0\varepsilon_1^{(1,p)}\varepsilon_2^{(2,tot)}. \quad (12)$$

Similar formulas can be written for the other three one-dimensional coincident peaks.

The difference between the spectrum of all events in the photopeak area and the one-dimensional coincident spectrum in the same area in a given detector is due to anticoincidence events, i.e. to the events when the second γ-ray is not detected. For detector 1, this difference, $N_{1ac}^{(1,p)}$, is given by

$$N_{1ac}^{(1,p)} = N_1^{(1,p)} - N_{1c}^{(1,p)} = N_0\varepsilon_1^{(1,p)}(1 - \varepsilon_1^{(2,tot)}) - N_0\varepsilon_1^{(1,p)}\varepsilon_2^{(2,tot)}$$
$$= N_0\varepsilon_1^{(1,p)}(1 - \varepsilon_1^{(2,tot)} - \varepsilon_2^{(2,tot)}) \quad (13)$$

Here, $(1-\varepsilon_1^{(2,tot)}-\varepsilon_2^{(2,tot)})$ is the probability that the second gamma is not detected by either detector.

Similar equations can be written for the three other anticoincidence peaks.

We can then calculate the ratio of experimental observables

$$\frac{1 - \varepsilon_1^{(1,tot)}}{1 - \varepsilon_1^{(1,tot)} - \varepsilon_2^{(1,tot)}} \equiv \frac{N_1^{(2,p)}}{N_{1ac}^{(2,p)}} = R_1^{(2,p)}, \quad (14)$$

and similar ratios for $R_1^{(1,p)} = N_1^{(1,p)}/N_{1ac}{}^{(1,p)}$, $R_2^{(1,p)} = N_2^{(1,p)}/N_{2ac}^{(1,p)}$, and $R_2^{(2,p)} = N_2^{(2,p)}/N_{2ac}^{(2,p)}$

Total detection probabilities $\varepsilon_i^{(j,tot)}(i = 1, 2; j = 1, 2)$ can be found from Eq. (14), for example

$$\varepsilon_1^{(1,tot)} = \frac{R_2^{(2,p)} - 1}{R_1^{(2,p)} + R_2^{(2,p)} - 1} \quad (15)$$

Using the results of Eq. (15), the photopeak detection probability of the first γ-ray in the first detector, $\varepsilon_1^{(1,p)}$, can be easily

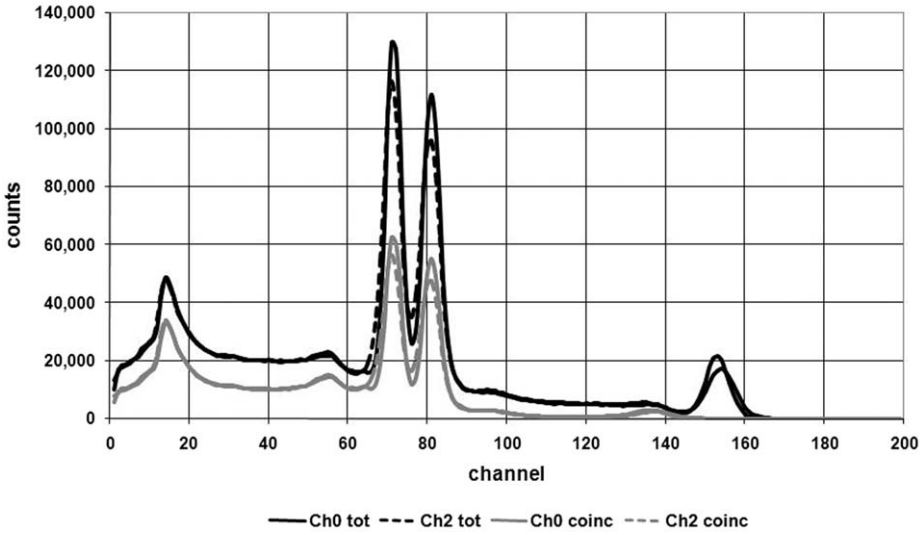

Fig. 2. One-dimensional spectra in the two detectors, both total and coincident. Channel 1 stands for the top detector, channel 2 stands for the bottom detector.

found from Eq. (12)

$$\varepsilon_1^{(1,p)} = \frac{N_{1c}^{(1,p)}}{N_0 \varepsilon_2^{(2,tot)}}, \tag{16}$$

and the photopeak detection probabilities for the other three combinations of γ-rays and detectors can be written in a similar form.

The decay rate N_0 can now be calculated in two ways

$$\bar{N}_0 = \frac{N_{1c}^{(1,p)} N_{2c}^{(2,p)}}{N_c^{(1,2)}} \frac{1}{\varepsilon_1^{(1,tot)} \varepsilon_2^{(2,tot)}} \tag{17a}$$

$$\tilde{N}_0 = \frac{N_{1c}^{(2,p)} N_{2c}^{(1,p)}}{N_c^{(2,1)}} \frac{1}{\varepsilon_1^{(2,tot)} \varepsilon_2^{(1,tot)}} \tag{17b}$$

where detection probabilities are given by Eqs. (15) and (16).

These two solutions can be rewritten in terms of observables similar to Eq. (6)

$$\bar{N}_0 = \frac{(N_1^{(2,p)} N_2^{(2,p)} - N_{1c}^{(2,p)} N_{2c}^{(2,p)})(N_1^{(1,p)} N_2^{(1,p)} - N_{1c}^{(1,p)} N_{2c}^{(1,p)})}{N_c^{(1,2)} (N_1^{(2,p)} - N_{1c}^{(2,p)})(N_2^{(1,p)} - N_{2c}^{(1,p)})} \tag{18a}$$

$$\tilde{N}_0 = \frac{(N_1^{(2,p)} N_2^{(2,p)} - N_{1c}^{(2,p)} N_{2c}^{(2,p)})(N_1^{(1,p)} N_2^{(1,p)} - N_{1c}^{(1,p)} N_{2c}^{(1,p)})}{N_c^{(2,1)} (N_1^{(1,p)} - N_{1c}^{(1,p)})(N_2^{(2,p)} - N_{2c}^{(2,p)})} \tag{18b}$$

The symmetric combination of Eqs. (18a) and (18b) gives the solution of the problem

$$N_0 = \sqrt{\bar{N}_0 \tilde{N}_0} \tag{19}$$

Eq. (19) was derived under the assumption that both γ-rays in ^{60}Co decay are emitted independently. In fact, however, this assumption is not valid. Both γ-rays are emitted in E2 type transitions with $\Delta J = 2$, $\Delta P = 0$. Because of this, the correlation function $W(\cos\theta)$ between γ-rays is an even function of $\cos\theta$, where θ is the angle between the two γ-rays (see [21])

$$W(\cos\theta) = 1 + a_2 P_2(\cos\theta) + a_4 P_4(\cos\theta) \tag{20}$$

where $P_n(\cos\theta)$ is a Legendre polynomial of n-th order. Since function $W(\cos\theta)$ is an even function of $\cos\theta$, if the source is located in the center of symmetry between the two identical detectors, the probabilities of the second gamma detection in the same or opposite detector are equal, and Eqs. (9)–(19) are still valid.

3. Experimental data and results

Experimental data were obtained with the NIST 203 mm (8 in.) NaI(Tl) coincidence detector, shown in Fig. 3.

Two NaI(Tl) crystals 203 mm (8 in.) in diameter and 152 mm (6 in.) thick are coupled with 127 mm PMTs. The sample cavity between the detectors is 127 mm in diameter and 38 mm in height. Detectors are placed inside a low-background chamber, however, for loading and unloading the source, they can be moved out of the chamber and opened using a pneumatic lift. Crystals and PMTs were recently upgraded; the passive shield and mechanical setup is the same as described in [22]. Detectors are connected to spectroscopic amplifiers and to a PIXIE-4 data acquisition module [23]. Pulses from both detectors are recorded and analyzed using IGOR software [24].[1]

Three ^{60}Co sources, previously calibrated with the 4πβ-γ method [25], were measured. Each source was measured in two positions inside the detector: (1) close to the center of the sample chamber and (2) placed at the bottom of the sample chamber. For each sample, three spectra were measured: spectra for the top and bottom detectors and a two-dimensional coincident spectrum. The background was subtracted channel-by-channel from all spectra. The number of channels in the spectra, recorded by PIXIE-4 in the energy interval from 0 to 3000 keV, was 20,000. Spectra were re-binned before data processing. In Fig. 1, a typical example of a two-dimensional ^{60}Co spectrum is shown.

Two-dimensional coincidence spectra projected onto the two axes, together with the total spectra measured by the two detectors, are shown in Fig. 2.

Note that the summation peak is missing in the coincident spectra because in this case, both γ-rays are detected by the same detector. As it was mentioned before, the difference between total and coincident spectra is the anticoincidence spectrum. The anticoincidence spectrum can also be obtained from the two-dimensional spectrum as the spectrum of events in one detector when the energy deposited in the other detector is zero.

[1] Certain commercial equipment, instruments, software, or materials are identified in this paper to specify adequately the experimental procedure. Such identification does neither imply recommendation or endorsement by the National Institute of Standards and Technology, nor does it imply that the materials or equipment identified are necessarily the best available for the purpose.

Fig. 3. The NIST NaI(Tl) coincident detector (a) open and (b) closed.

Table 1
Results for activities of three ^{60}Co sources by the method explained in this paper, measured in the middle and bottom positions inside the sample chamber.

Source	Position	Measurement time (s)	Count rate (s^{-1})	Counts (background subtracted)	Calculated activity (Bq)	Difference middle/bottom (%)
C5	Middle	1934.4	3618.4	6908312	3099.3	0.8
	Bottom	1922.3	3641.2	6908778	3074.4	
C3	Middle	3217.3	2175.6	6848618	1835.1	0.9
	Bottom	3196.2	2190.0	6849511	1817.9	
C1	Middle	8578.1	815.98	6598115	665.2	1.7
	Bottom	8530.6	820.52	6600324	653.6	

The 1173 and 1332 keV peaks in total, non-coincident spectra and in one-dimensional coincident spectra were fitted by the sum of the two Gaussian curves and a constant C. The constant C for total and non-coincident spectra was chosen to be the same and was found from spectra in the high-energy area, where the contribution from the summation peak is zero. For one-dimensional coincident spectra, the constant C was put to zero. The number of degrees of freedom for a one-dimensional fit was about 350.

Summation peaks in both total and non-coincident spectra were fitted by a Gaussian curve. The approximate number of degrees of freedom for a summation peak fit was close to 300.

The two-dimensional peaks were fitted by a two-dimensional Gaussian distribution. Each two-dimensional photopeak fit had about 20,000 degrees of freedom.

Table 1 shows activities of sources calculated using Eq. (19) for the two positions of each source. It is seen that the results practically do not depend on the position. At the same time, as seen from Table 2, the detection probabilities do depend on position.

In the comparison in Table 3, the results obtained by the γ–γ coincident measurements are in good agreement with the results obtained for the same samples by the $4\pi\beta$-γ method.

A detailed uncertainty budget is given in Table 4.

Table 2
Detection probabilities measured in two different positions for three sources.

Source	Position	$\varepsilon_1^{(1,p)}$	$\varepsilon_1^{(1,tot)}$	$\varepsilon_1^{(2,p)}$	$\varepsilon_1^{(2,tot)}$	$\varepsilon_2^{(1,p)}$	$\varepsilon_2^{(1,tot)}$	$\varepsilon_2^{(2,p)}$	$\varepsilon_2^{(2,tot)}$
C5	Middle	0.163	0.346	0.162	0.348	0.162	0.322	0.149	0.321
	Bottom	0.124	0.280	0.124	0.281	0.218	0.409	0.201	0.408
C3	Middle	0.162	0.342	0.162	0.344	0.168	0.327	0.153	0.326
	Bottom	0.129	0.272	0.122	0.278	0.226	0.421	0.210	0.412
C1	Middle	0.162	0.341	0.161	0.346	0.169	0.320	0.153	0.326
	Bottom	0.126	0.274	0.123	0.279	0.227	0.421	0.210	0.413

Table 3
Comparison of γ–γ and $4\pi\beta$-γ measurements.

Source	Gamma–gamma (Bq)	Beta–gamma (Bq)
C5	3099 ± 14	3101 ± 6
C3	1835.1 ± 8.1	1831.5 ± 3.6
C1	665.2 ± 2.9	656.4 ± 1.3

The activities of three ^{60}Co sources measured by the gamma–gamma coincident method are the activities of samples in the middle position. Uncertainties correspond to one standard deviation ($k = 1$).

Table 4
Uncertainty budget.

Input quantity x_i ,the source of uncertainty (and individual uncertainty components where appropriate)	Method used to evaluate $u(x_i)$, the standard uncertainty of x_i (A) denotes evaluation by statistical methods (B) denotes evaluation by other methods	Relative uncertainty of input quantity, $u(x_i)/x_i$, (%)	Relative sensitivity factor, $\lvert\partial y/\partial x_i\rvert$ (x_i/y)	Relative uncertainty of output quantity, $u_i(y)/y$, (%)
Number of counts in 1D peaks	Statistical (A)	0.18	1.0	0.18
Number of counts in 2D peaks	Statistical (A)	0.25	1.0	0.25
Uncertainty in subtraction constant C	Estimated (B)	5	0.06	0.3
Uncertainty in the dead time corrections	Estimated (B)	0.075	1	0.075
Difference in two methods of activity calculations: Eqs. (18a) and (18b)	Estimated (B)	0.08	1.0	0.08
Combined relative standard uncertainty of the evaluation				**0.44**

Acknowledgements

This material is based upon the activities supported by the National Science Foundation under Agreement no. PHY-0453430. Any opinions, findings and conclusions or recommendations expressed are those of the author(s) and do not necessarily reflect the views of the National Science Foundation.

The authors are grateful to Ryan Fitzgerald for samples, measurements performed by the $4\pi\beta$-γ method and numerous discussions. We are also grateful to Jerry LaRosa, Robin Hutchinson, and Mike Unterweger for support and discussions.

References

[1] NCRP Report 58, A handbook of radioactivity measurements NCRP, 1985.
[2] G.F. Knoll, Radiation Detection and Measurement, third edition, Wiley, New York, 2000.
[3] S. Pommé, Metrologia 44 (2007) S17.
[4] J.S. Eldridge, P. Crowther, Nucleonics 22 (1964) 56.
[5] J.G.V. Taylor, X-ray–X-ray coincidence counting methods for the standardization of ^{125}I and ^{197}Hg in Standardization of Radionuclides, IAEA, Vienna, 1967, pp. 341–355.
[6] D.L. Horrocks, P.R. Klein, Nucl. Instr. and Meth. 124 (1975) 585.
[7] H. Schrader, K.F. Walz, Appl. Radiat. Isot. 38 (1987) 763.
[8] R.H. Martin, J.C.V. Taylor, Nucl. Instr. and Meth. A 312 (1992) 64.
[9] J.M. Lee, K.B. Lee, M.K. Lee, et al., Appl. Radiat. Isot. 60 (2004) 397.
[10] S. Pommé, T. Altzitzoglou, R. Van Ammel, G. Sibbens, Nucl. Instr. and Meth. A 544 (2005) 584.
[11] P. Shapiro, R.W. Higgs, Rev. Sci. Instrum. 28 (1957) 939.
[12] R.W. Hayward, D.D. Hoppes, W.B. Mann, J. Res. NBS 54 (1955) 47.
[13] G.A. Brinkman, A.H.W. Aten Jr., J.T. Veenboer, Int. J. Appl. Radiat. Isot. 14 (1963) 153.
[14] G.A. Brinkman, A.H.W. Aten Jr., J.T. Veenboer, Int. J. Appl. Radiat. Isot. 14 (1963) 433.
[15] G.A. Brinkman, A.H.W. Aten Jr., J.T. Veenboer, Int. J. Appl. Radiat. Isot. 16 (1963) 15.
[16] Evaluated Nuclear Structure Data File (ENSDF), 2009, 〈http://www.nndc.bnl.gov/ensdf/〉.
[17] J.M.R. Hutchinson, W.B. Mann, P.A. Mullen, Nucl. Instr. and Meth. 112 (1973) 187.
[18] T. Kawano, H. Ebihara, Appl. Radiat. Isot. 41 (1990) 163.
[19] T. Kawano, H. Ebihara, Appl. Radiat. Isot. 42 (1991) 1165.
[20] I.J. Kim, C.S. Park, H.D. Choi, Appl. Radiat. Isot. 58 (2003) 227.
[21] R.D. Gill, Gamma-Ray Angular Correlations, Academic Press Inc., London, 1975.
[22] J.M.R. Hutchinson, et al., IEEE Trans. Nucl. Sc. NS-19 (1972) 117.
[23] 〈http://www.xia.com/index.html〉.
[24] 〈http://www.wavemetrics.com/〉.
[25] R. Fitzgerald, M.K. Schultz, Appl. Radiat. Isot. 66 (2008) 937.